



Acetaldehyde and acetone in the Arctic snowpack during the ALERT2000 campaign. Snowpack composition, incorporation processes and atmospheric impact

Stéphan Houdier^a, Sébastien Perrier^a, Florent Dominé^{a,*}, Axel Cabanes^a,
Loïc Legagneux^a, Amanda M. Grannas^b, Christophe Guimbaud^b,
Paul B. Shepson^{b,c}, Hacene Boudries^d, Jan W. Bottenheim^d

^a CNRS, Laboratoire de Glaciologie et Géophysique de l'Environnement, BP 96, 54 rue Molière,
38402 Saint Martin d'Hères Cédex, France

^b Department of Chemistry, Purdue University, West Lafayette, IN 47907-1393, USA

^c Department of Earth and Atmospheric Sciences, Purdue University, West Lafayette, IN 47907-1393, USA

^d Meteorological Service of Canada, 4905 Dufferin Street, Toronto, Ontario, Canada M3H 5T4

Received 12 June 2001; received in revised form 27 November 2001; accepted 11 January 2002

Abstract

Acetaldehyde and acetone were measured in the seasonal snowpack near Alert (Nunavut, Canadian Arctic) in February and April 2000. Acetaldehyde concentrations in fresh surface snow in February were about 2.5 ppbw, decreasing to 1 ppbw after several days, while gas-phase acetaldehyde was about 75 pptv. Values for aged layers were 1.3–2.6 ppbw. In April, values for fresh snow were 5–10 ppbw, decreasing to 1–4 ppbw after several days (gas-phase values were around 230 pptv). Values for aged layers were in the range 0.7–3 ppbw. Snow-phase acetaldehyde represented 67% of the (snow + atmospheric mixing layer) system in winter and 94% in spring. Preliminary acetone measurements yielded values 1.5–3 ppbw in surface snow several days after deposition. To understand the kinetics of exchange of acetaldehyde between the air and the snow, its mechanism of incorporation in snow was investigated. Surface incorporation by adsorption, and volume incorporation by dissolution were considered. Winter and spring measurements showed very different trends, and spring concentrations were higher than winter ones, which is contrary to thermodynamic expectations. The photolytical production of acetaldehyde in the snowpack is proposed as an explanation. © 2002 Elsevier Science Ltd. All rights reserved.

Keywords: Acetaldehyde; Acetone; Snow; Incorporation processes; ALERT2000

1. Introduction

Low molecular weight aldehydes (RH(C=O)) and ketones (RR'(C=O)) are ubiquitous volatile organic compounds in the Arctic atmosphere (Barrie et al., 1988; Bottenheim et al., 1990; De Serves, 1994; Shepson et al., 1996). Recent observations that formaldehyde (HCHO), acetaldehyde (CH₃CHO) and acetone ((CH₃)₂CO) were elevated in snowpack interstitial air (Couch et al., 2000)

and that NO_x was photochemically produced in the snowpack (Honrath et al., 1999) indicate that the snowpack is chemically active and that it can release carbonyl compounds to the troposphere. Such a source may explain why their Arctic tropospheric concentrations cannot be explained by considering only (i) gas-phase oxidation of hydrocarbons as the main source and (ii) photolysis and radical oxidation as the main sinks (Shepson et al., 1996; Sumner and Shepson, 1999).

Although gas-phase formaldehyde (Bottenheim et al., 1990; De Serves, 1994; Shepson et al., 1996; Sumner and Shepson, 1999; Hutterli et al., 1999), acetaldehyde and

*Corresponding author. Tel.: +33-476-82-42-69.

E-mail address: florent@glaciog.ujf-grenoble.fr (F. Dominé).

acetone (Yokouchi et al., 1994; Shepson et al., 1996) have been measured in the Arctic, only formaldehyde has been measured in the snow-phase (Sumner and Shepson, 1999; Hutterli et al., 1999). One reason for this is the lack of an analytical method able to measure the very low concentrations expected for acetaldehyde, acetone, and other carbonyls in polar snow. Here we report the first measurements of CH_3CHO and $(\text{CH}_3)_2\text{CO}$ in Arctic snow, using the novel method described in Houdier et al. (2000). These measurements were performed at Alert (Nunavut, Canadian Arctic, $82^\circ 29.94'\text{N}$, $62^\circ 20.55'\text{W}$) during the ALERT2000 field campaign. Our goals were to determine the partitioning and to understand the mechanism of exchange of light carbonyls between the atmosphere and the snowpack. This required the investigation of the incorporation mechanism of carbonyls in snow, which we attempt to elucidate to facilitate the parameterization of air–snow interactions in atmospheric chemistry models.

2. Methods

2.1. Sampling and stratigraphy

All measurements were conducted from 8 to 20 February (winter campaign) and from 12 April to 1 May (spring campaign). Analyses were performed in the FTX building ($82^\circ 27.28'\text{N}$, $62^\circ 29.69'\text{W}$), located on a plateau $\approx 180\text{ m a.s.l.}$ and 5.4 km SW of the Alert base. The main sampling site was 300 m SE of the FTX

building and is hereafter identified as site A. Sampling there was done at several locations having similar stratigraphies and being distant by only a few meters. Some samples were also collected 10 m South of the FTX building (hereafter: FTX site).

Snow layers were separated into two types: recent surface snow and deeper, aged snow layers, because the compositions of aged layers were found to be fairly stable, while those of surface layers varied rapidly with time. Surface layers were designated by their dates of deposition (e.g. 3 February snowfall). For convenience, layers were numbered from bottom to top, with the letter W or S referring to the winter or spring snowpack, respectively. The winter and spring snow stratigraphies at site A are reported in Table 1. Additional details are found in Dominé et al. (2002). The surface layers studied were the 3 February (3W) and 7 February (4W) snowfalls in the winter campaign and the 13–14 April (7S) and 25–28 April (8S) snowfalls in the spring campaign, as well as both thin snow layers deposited a few days or weeks before the spring campaign, hereafter called crusted (6S) and loose (5S) surface snow layers. These surface snow layers were sampled every 1 or 2 days. Deeper snow layers (1W, 2W and 1S–4S layers) were sampled less frequently.

2.2. Analytical procedure

Formaldehyde, acetaldehyde, and acetone in melted snow were measured using DaNSyl-Acetamido-Oxy-Amine (DNSAOA) as derivatizing agent (Houdier

Table 1

Total acetaldehyde in the winter snowpack, before 22 February, and in the spring snowpack, before layer 8S formed on 25–28 April

Snow layer	Layer number	Thickness (cm)	Density (g cm^{-3})	$[\text{CH}_3\text{CHO}]_{\text{snow}}$ (ppbw)	CH_3CHO Snowpack loading (ng cm^{-2})	Contribution (%)
<i>Winter snowpack</i>						
7 February fall	4W	1	0.08	1	0.08	0.81
3 February fall	3W	1.5	0.15	1	0.225	2.28
Hard	2W	15	0.48	1	7.2	72.87
Depth hoar	1W	8	0.22	1.35	2.376	24.05
Total		25.5			9.9	100
<i>Spring snowpack</i>						
13–14 April fall	7S	0.3	0.16	4.5	0.216	1.16
Crusted	6S	1	0.16	4	0.64	3.43
Loose	5S	1.5	0.16	3.8	0.912	4.89
Semi-hard	4S	10	0.4	1.7	6.8	36.48
Soft	3S	5	0.3	1.7 ^a	2.55	13.68
Hard	2S	12	0.48	1	5.76	30.90
Depth hoar	1S	8	0.2	1.1	1.76	9.44
Total		37.8			18.6	100

^aNot measured. Concentration assumed to be identical to semi-hard snow.

et al., 2000). The oxime ethers formed were separated by reversed-phase high performance liquid chromatography (HPLC) and detected by fluorescence spectroscopy. The analytical reproducibility, mainly determined by the uncertainty in determining the slope of the calibration curve, was better than 20%. The detection limit for each carbonyl was 0.1–0.3 ppbw depending on the initial purity of the DNSAOA reacting solution.

2.3. Snow chemical heterogeneity and contamination

To detect a possible spatial heterogeneity of the snow, each layer was sampled at least three times (up to six times). Most triplicate samples were characterized by homogeneous HCHO concentrations (Perrier et al., 2002) but strong variations were often observed for CH₃CHO, which are attributed to contamination while preparing the reacting solution. Data therefore had to be filtered. Contamination appeared to be random and to affect 30–40% of samples. A limit was set on the maximum variability within a set of triplicate samples. Somewhat arbitrarily, we rejected values that were more than 1.3 times higher than the lowest value of a given set of samples. It is possible that all three samples from the same sampling were contaminated. Time series of [CH₃CHO]_{snw} displayed trends, and values more than 50% greater than the general trend were rejected. Positive error bars shown are the standard deviation. When only one data point was retained, no positive error bar is reported. Negative error bars are difficult to determine when there is contamination. Here, they are the difference between the highest and lowest non-rejected values. When only one point was used, the negative error bar was the difference between the retained value and the lowest non-retained value. This does not fully respect the actual definition of error bars, but it is meant to give an idea of the extent of contamination, which is a greater source of uncertainty than usual instrumental errors.

3. Results

3.1. Acetaldehyde in the snowpack: concentration and evolution

3.1.1. Aged snow layers

Two aged layers, i.e. depth hoar (1W) and hard wind-packed (2W), were identified during the winter campaign (Dominé et al., 2002). These layers were still present in spring (1S and 2S), when two additional layers, (3S) and (4S), were also observed. The [CH₃CHO]_{snw} data for these layers are given in Table 2. The value of 1.15 ppbw measured for depth hoar in April (1S layer) is similar to those measured in winter, 1.36 and 1.37 ppbw, suggesting that the composition of this layer was homogeneous and that it did not change between both campaigns. Its homogeneity may be due to the intense water vapor remobilization needed to form depth hoar (Marbouty, 1980). The seasonal difference observed for hard snow (2W and 2S layers) is probably due to the strong spatial variability of this snow layer, which was formed by several precipitation and wind blowing events (Dominé et al., 2002). This is supported by observations of large standard deviations in HCHO and ionic concentrations observed in this layer (Perrier et al., 2002; Dominé et al., 2002). [CH₃CHO]_{snw} in the semi-hard (4S) layer were in the range 1.5–3 ppbw.

3.1.2. Surface snow layers

The time evolution of [CH₃CHO]_{snw} in surface layers are reported in Figs. 1–3. The evolutions of the specific surface area (SSA) of the snow are also reported to facilitate the discussion of the incorporation mechanism of CH₃CHO in snow.

[CH₃CHO]_{snw} in the 7 February layer (4W, Fig. 1), decreased from ~2 to ~1 ppbw within the first 5 days following the first sampling, on 9 February. After this initial decrease, a steady-state concentration of about 1 ppbw was reached. The slightly higher value of 18

Table 2
Acetaldehyde concentrations in deep layers at site A

Snow layer	Layer number	Sampling date	[CH ₃ CHO] _{snw} (ppbw)	Positive error bar (ppbw)	Negative error bar (ppbw)
Hard	2W	9 February	2.36	0.08	0.11
Depth hoar	1W	10 February	1.36	0.16	0.23
Depth hoar	1W	13 February	1.37	0.23	0.23
Semi-hard	4S	14 April	2.05	0.13	0.19
Semi-hard	4S	14 April	1.51		0.49
Hard	2S	14 April	1.05	0.11	0.2
Semi-hard	4S	21 April	2.96	1.22	1.22
Hard	2S	21 April	0.66	0.06	0.09
Depth hoar	1S	21 April	1.15	0.16	0.31

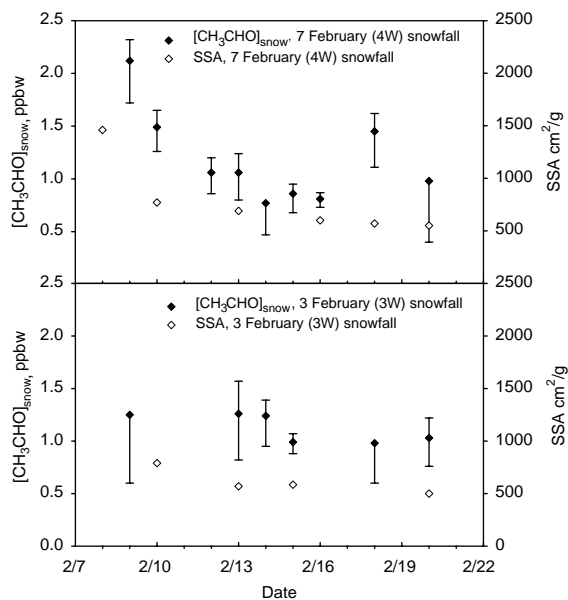


Fig. 1. $[\text{CH}_3\text{CHO}]_{\text{snow}}$ (closed symbols) and specific surface area (SSA, open symbols) for the 7 February snowfall (4W layer, top panel) and for the 3 February snowfall (3W layer, bottom panel). Samples were collected at site A.

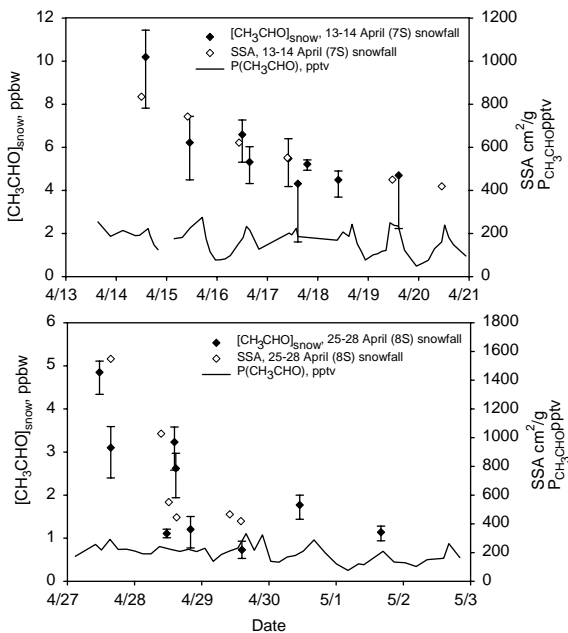


Fig. 2. $[\text{CH}_3\text{CHO}]_{\text{snow}}$ (closed symbols) and SSA (open symbols) for the 13–14 April snowfall (7S layer, top panel) and for the 25–28 April snowfall (8S layer, bottom panel). Samples were collected at site A.

February could be due to a slight contamination. The observed decrease suggests an initial concentration of $\sim 3.5\text{--}4$ ppbw just after deposition. The formation of

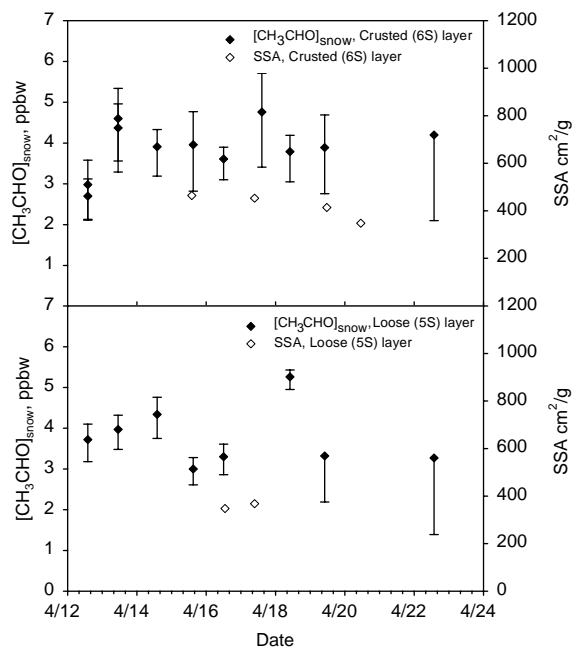


Fig. 3. $[\text{CH}_3\text{CHO}]_{\text{snow}}$ (closed symbols) and SSA (open symbols) for the crusted layer (6S layer, top panel) and for the loose layer (5S layer, bottom panel). Samples were collected at site A.

surface hoar on top of the 4W layer began to be visible on 13 February. Cabanes et al. (2002) estimate that surface hoar accounted for about 10%, 25% and 50% of the mass of this layer on 13, 18 and 20 February, respectively. Since $[\text{CH}_3\text{CHO}]_{\text{snow}}$ did not change much between 13 and 20 February, we assume that $[\text{CH}_3\text{CHO}]_{\text{snow}}$ for surface hoar was close to 1 ppbw. This is supported by the analysis of hoar frost growing on guy wires, that had 1.3 ppbw of CH_3CHO . The 3 February (3W) snowfall was first sampled 6 days after its deposition: at that time $[\text{CH}_3\text{CHO}]_{\text{snow}}$ had already reached a steady-state value of also about 1 ppbw (Fig. 1).

Similar trends can be observed in Fig. 2 for both spring snowfalls: 13–14 April (7S) and 25–28 April (8S) layers. $[\text{CH}_3\text{CHO}]_{\text{snow}}$ decreased from ~ 10 to $\sim 4\text{--}5$ ppbw within the first 4 days after the 13–14 April snowfall (Fig. 2, top). As already observed for the 4W layer, surface hoar progressively grew on top of the 13–14 April (7S) layer. Dominé et al. (2002) estimate that surface hoar made up about 25% and 80% of the mass of this layer on 17 and 19 April, respectively. Again, as $[\text{CH}_3\text{CHO}]_{\text{snow}}$ did not change significantly between these two dates, we assume that $[\text{CH}_3\text{CHO}]_{\text{snow}}$ for surface hoar was near 4 ppbw. Although the 25–28 April snowfall (8S) episode was very complex (variable wind speed and direction, riming, rapid modification of the snow crystal shapes after deposition, see Cabanes et al., 2002), $[\text{CH}_3\text{CHO}]_{\text{snow}}$ shows a similar trend,

decreasing from about 5 ppbw to about ~ 1.5 ppbw in a few days (Fig. 2, bottom). As observed also for HCHO (Perrier et al., 2002), initial and steady-state $[\text{CH}_3\text{CHO}]_{\text{snow}}$ measured during this episode were about half of that observed for the 7S layer. This episode was characterized by higher temperatures ($T = -15^\circ\text{C}$) and by a rapid drop of HCHO and CH_3CHO mixing ratios associated with ozone destruction by bromine chemistry (Bottenheim et al., 2002).

In the period between 12 and 22 April, almost constant $[\text{CH}_3\text{CHO}]_{\text{snow}}$ were measured in both subsurface layers (5S) and (6S) (Fig. 3). Although the dates of deposition of these layers is unknown, Dominé et al. (2002) estimate that they were several days to 2 weeks old at the beginning of the sampling period and had probably achieved, on 12 April (first sampling), the evolution that we observed for fresh snow. We also note that the ~ 4 and ~ 3.5 ppbw mean concentrations measured for 6S and 5S layers, respectively, are comparable to the steady-state concentration measured in the 7S layer several days after the 13–14 April snowfall.

In summary, $[\text{CH}_3\text{CHO}]_{\text{snow}}$ in surface layers decrease rapidly within 3–5 days after the snowfall to reach a steady-state concentration of ~ 1 ppbw in the winter and, except during low ozone episodes, 3.5–4 ppbw in the spring. Interestingly, these decreasing trends resemble those observed for HCHO at Summit, Greenland, in summer (Hutterli et al., 1999) and at Alert in the spring during this campaign (Perrier et al., 2002). Note, however, that in winter HCHO measurements do not indicate such an initial decrease (Perrier et al., 2002), while CH_3CHO measurements do.

3.2. Acetone in the snowpack: preliminary results

To the best of our knowledge, acetone has never been measured in snow. Acetone is less reactive than light aldehydes with derivatization agents used. Here, reaction times of at least 5–7 days were required (Houdier et al., 2000) and only a few samples were analyzed

during the spring campaign, to yield preliminary data (Table 3).

Concentrations in surface snow, in the range 1.5–3.1 ppbw, seem to be higher at the FTX than at site A. High values were also recorded at this site for CH_3CHO but each set of samples was characterized by a very strong variability that forced us to discard those data. A contamination caused by the proximity of the building is possible, although it was not observed for HCHO. The snowpack at the FTX was much thicker than at site A, because of wind effects around the building. This may have affected acetone concentrations, but our understanding of acetone–snow interactions is not sufficient to elaborate on this point. As illustrated by the relatively low standard deviation, no contamination was encountered for acetone. Interestingly, the FTX data suggest a slightly higher nighttime concentration in surface snow, but data are too sparse and this observation will need further confirmation.

4. Discussion

4.1. Acetaldehyde snowpack loading and snow-boundary layer partitioning

By using the mean thickness, densities and steady-state $[\text{CH}_3\text{CHO}]_{\text{snow}}$ of the different layers, the total acetaldehyde loading per surface unit of the snowpack was calculated, and found to be 10 and 19 ng cm^{-2} of snow in winter and spring, respectively (Table 1). Surface snow layers, which may exchange more rapidly with the atmosphere, contribute only $\sim 3\%$ and $\sim 9\%$ to the total loading of the snowpack in winter and spring, respectively.

The partitioning of CH_3CHO between the atmospheric mixing layer (ML) and the snowpack can be determined from our data and gas-phase measurements. For a highly stable atmosphere such as that generally observed during ALERT 2000, the height of the ML for CH_3CHO can be approximated by the vertical distance the molecule can diffuse in one lifetime (Guimbaud et al.,

Table 3
Acetone concentrations in surface snow layers in the spring. Time is EST (GMT-5)

Snow layer	Layer number	Sampling site	Sampling date	$[(\text{CH}_3)_2\text{CO}]_{\text{snow}}$ (ppbw)	Standard deviation
Crusted	6S	A	12 April, 15:00	1.61	0.10
Loose	5S	A	12 April, 15:00	1.51	0.05
Loose	5S	A	12 April, 16:00	1.62	0.11
13–14 April fall	7S	FTX	19 April, 14:30	2.55	0.15
Crusted	6S	FTX	19 April, 14:30	2.00	0.14
13–14 April fall	5S	FTX	20 April, 3:30	2.70	0.37
Crusted	6S	FTX	20 April, 3:30	3.05	0.25

2002). As discussed by Guimbaud et al. (2002), assuming an atmospheric lifetime of 19 h and an eddy diffusivity coefficient $K_z = 95 \text{ cm}^2 \text{ s}^{-1}$, the mixing height was $H = 25 \text{ m}$ for CH_3CHO in mid-April. In the dark period the lifetime of CH_3CHO , mainly determined by physical removal processes, is longer than several tens of days, which allows the mixing of CH_3CHO within the winter inversion layer. The spring-time height of the inversion layer at Alert was 400 m (Guimbaud et al., 2002). In the winter, convection is reduced because the atmospheric temperature gradient is stronger, and we postulate a 300 m thick ML in winter. Assuming homogeneous $P_{\text{CH}_3\text{CHO}}$ throughout the ML, and using mean values of 74 ppt ($P_{\text{tot}} = 1 \text{ atm}$, $T_{\text{mean}} = 238 \text{ K}$; Guimbaud et al., 2002) in winter and 228 ppt in spring ($P_{\text{tot}} = 1 \text{ atm}$, $T_{\text{mean}} = 248 \text{ K}$; Boudries et al., 2002), we calculated that 67% and 94% of the CH_3CHO in the (snow + ML) system was in the snowpack in winter and spring, respectively. Most of the CH_3CHO in the (snow + ML) system is then sequestered in snow. Even in the absence of chemical production in the snowpack, physical exchanges of CH_3CHO between the snow and the ML has the potential to impact lower tropospheric chemistry. Understanding and quantifying these potential exchanges requires the understanding of the mechanisms of incorporation of CH_3CHO in snow.

4.2. Incorporation mechanisms of acetaldehyde in snow

4.2.1. Mechanism assumptions

Acetaldehyde in snow can be incorporated either by (i) adsorption onto the surface of precipitating snow crystals; (ii) dissolution in the ice volume with the formation of a solid solution at thermodynamic equilibrium (SSE); (iii) dissolution into the ice volume governed by kinetic processes, rather than equilibrium; (iv) a combination of several of the above three mechanisms (Dominé et al., 1995; Dominé and Thibert, 1996; Bales and Choi, 1996; Thibert and Dominé, 1997, 1998). These mechanisms lead to three different equations that relate the mole fraction of CH_3CHO in snow ($X_{\text{CH}_3\text{CHO}}$) to other chemical and physical parameters. These equations are listed below, and the reader is referred to Perrier et al. (2002) for details regarding their derivation. Eqs. (1)–(3) apply to mechanisms (i), (ii) and (iii), respectively,

$$X_{\text{CH}_3\text{CHO}} = A \text{ SSA} (P_{\text{CH}_3\text{CHO}})^{1/n} \exp\left(\frac{\Delta H_{\text{ads}}}{nRT}\right), \quad (1)$$

$$X_{\text{CH}_3\text{CHO}} = A' (P_{\text{CH}_3\text{CHO}})^{1/n'} \exp\left(\frac{\Delta H_{\text{sub}}}{n'RT}\right), \quad (2)$$

$$X_{\text{CH}_3\text{CHO}} = \frac{P_{\text{CH}_3\text{CHO}}}{P_{\text{H}_2\text{O}}} \frac{\alpha_{\text{CH}_3\text{CHO}}}{\alpha_{\text{H}_2\text{O}}} \sqrt{\frac{M_{\text{H}_2\text{O}}}{M_{\text{CH}_3\text{CHO}}}}, \quad (3)$$

where T is temperature, SSA the specific surface area of snow, $P_{\text{CH}_3\text{CHO}}$ the CH_3CHO partial pressure, A and A' constants, n and n' the number of entities created by the adsorption/dissolution of CH_3CHO on/in the ice surface/volume (Thibert and Dominé, 1997), ΔH_{ads} and ΔH_{sub} the molar enthalpies of adsorption and sublimation of CH_3CHO on/from ice, α is its mass accommodation coefficients on ice and M its molar masses. Each possible mechanism can be tested using Eqs. (1)–(3).

4.2.2. Adsorption

This hypothesis was tested by plotting, following Eq. (1), $\text{Ln}([\text{CH}_3\text{CHO}]_{\text{snow}} / (P_{\text{CH}_3\text{CHO}} \times \text{SSA}))$ as a function of $1/T$ (Fig. 4). If CH_3CHO is located on the surface of ice crystals then, assuming linear adsorption isotherms, the plot must be linear. Because CH_3CHO is not expected to dissociate on the ice surface we assumed $n = 1$ in the calculations, implying that CH_3CHO does not create defects on the ice surface (Thibert and Dominé, 1997). Assuming that equilibration with the atmosphere occurs within 1–2 h or less, all the surface snow-phase $[\text{CH}_3\text{CHO}]_{\text{snow}}$ data obtained were used. When sampling times for $P_{\text{CH}_3\text{CHO}}$ and $[\text{CH}_3\text{CHO}]_{\text{snow}}$ were < 1 h apart, the data point for $P_{\text{CH}_3\text{CHO}}$ (Boudries et al., 2002) closest to the sampling time was used. Otherwise, 24 h averaged $P_{\text{CH}_3\text{CHO}}$ values were used. A constant $P_{\text{CH}_3\text{CHO}}$ value of 74 pptv (the average value of the less numerous winter data) was used for winter (Guimbaud et al., 2002). Temperatures, measured at the GAW laboratory, 460 m South of the FTX building, were averaged over the hour that preceded sampling. SSA values at the time of snow sampling were interpolated from the data shown here.

Fig. 4 shows that this hypothesis gives a linear fit with a good correlation coefficient ($R^2 = 0.70$, 40 data points) with spring data only. A molar enthalpy of adsorption of $\Delta H_{\text{ads}} = -58.2 \text{ kJ mol}^{-1}$ is derived from the slope of the least-square fit. ΔH_{ads} of CH_3CHO on ice is unknown but the value of $-58.2 \text{ kJ mol}^{-1}$ found here is fairly close to that determined by Schaff and Roberts (1998) for $(\text{CH}_3)_2\text{CO}$ at 140 K: -40 kJ mol^{-1} . Picaud et al. (2000), using molecular dynamics at 0 K, obtained ΔH_{ads} (acetone on ice) = -49 kJ mol^{-1} . Acetaldehyde is more polar than acetone and a slightly higher energy is reasonable and could be explained by 2–3 H-bonds. Considering spring data alone, adsorption then appears to be a reasonable mechanism to explain the incorporation of CH_3CHO in snow.

This hypothesis breaks down when the lower winter values are added to the spring data, and using all data yielded $R^2 = 0.12$ with 67 data points. Furthermore, Fig. 4 shows no correlation by considering winter data only, possibly because the temperature range in winter was narrower than in spring. Another reason may be because $P_{\text{CH}_3\text{CHO}}$ were not as well known in winter. Thus, one cannot definitely rule out that winter data

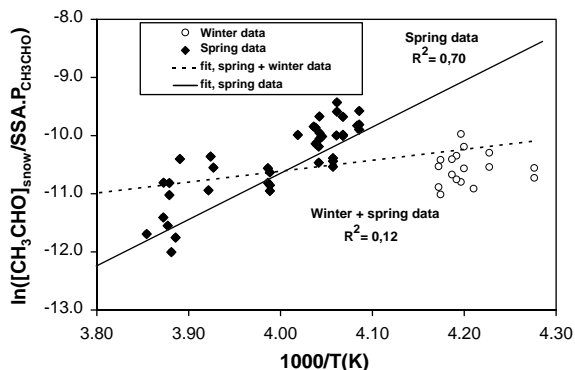


Fig. 4. Arrhenius-type plot to test the adsorption hypothesis. We assumed $n = 1$. $P_{\text{CH}_3\text{CHO}}$ data were from Boudries et al. (2002). $P_{\text{CH}_3\text{CHO}}$ in winter was assumed to be constant at 74 pptv. Temperatures, 1 h averaged, were measured at the GAW laboratory. SSA values at the time of sampling were interpolated from the data of Cabanes et al. (2002). Closed diamonds are the April data. Open circles are the February data. The solid line is the linear regression curve for April data. The dashed line is the linear regression curve for both April and February data.

alone would have shown a reasonable linear fit. Figs. 1–3 also show that $[\text{CH}_3\text{CHO}]_{\text{snow}}$ is correlated with SSA, which does suggest that adsorption may be involved.

Nevertheless, the winter data of Fig. 4 are far removed from the spring least-square fit. This suggests that either different incorporation mechanisms are involved in winter and spring or/and that there is an additional spring-time source of CH_3CHO in snow.

4.2.3. Solid solution at equilibrium (SSE)

To test for the SSE hypothesis (Eq. (2)) we have plotted in Fig. 5 $\ln([\text{CH}_3\text{CHO}]_{\text{snow}}/P_{\text{CH}_3\text{CHO}})$ as a function of $1/T$. We used $n' = 1$ in the calculations. Long equilibration times are required for volume processes. Even though the diffusion coefficient of CH_3CHO in ice, D , has never been measured, data exist for other molecules. Those of HCl and HNO_3 (Thibert and Dominé, 1997, 1998) and the self-diffusion of water in ice (Hobbs, 1974) are in the range 10^{-12} – $10^{-10} \text{ cm}^2 \text{ s}^{-1}$ for the temperatures of interest here, and we assume that D falls within this range. The diameter of the hollow columns and bullets of the snow falls of the 3 February (3W) and of 13–14 April (7S) layers were about 50–80 μm , (Dominé et al., 2001; Cabanes et al., 2002) so that the diffusion distance for equilibration was about $x = 30 \mu\text{m}$. The time constant for diffusion, given as $t = x^2/D$, was then 1–100 days, depending on the value of D .

Volume equilibration will then be much longer than surface equilibration and only steady-state values of $[\text{CH}_3\text{CHO}]_{\text{snow}}$ were selected for the plot of Fig. 5. $P_{\text{CH}_3\text{CHO}}$ and T were 24 h averaged to account for the

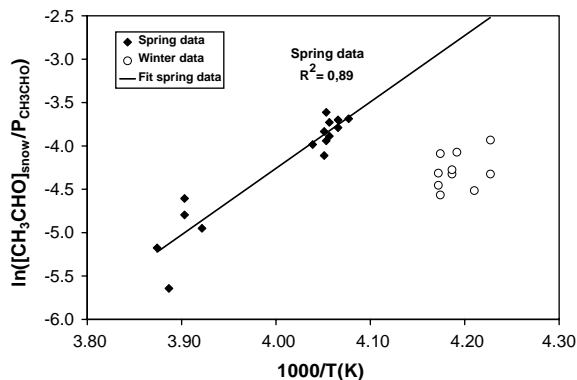


Fig. 5. Arrhenius-type plot for SSE hypothesis calculated by using steady-state $[\text{CH}_3\text{CHO}]_{\text{snow}}$, 24 h averaged $P_{\text{CH}_3\text{CHO}}$ and T and $n = 1$. Closed diamonds are the April data. Open circles are the February data. The solid line is the linear regression curve for April data.

long equilibration time scales. As in Fig. 4, this hypothesis gives a linear fit with a good R^2 coefficient ($R^2 = 0.89$, 20 data points) with spring data. This good correlation is lost when winter data are included ($R^2 = 0.13$, 30 data points). $\Delta H_{\text{sub}}(\text{CH}_3\text{CHO from ice}) = 67 \text{ kJ mol}^{-1}$ can be derived from the spring plot. Thibert and Dominé (1997, 1998) observed that, for HCl and HNO_3 , partial molar enthalpies of evaporation from water, ΔH_{evap} , and partial molar enthalpies of sublimation from ice, ΔH_{sub} , were fairly close. For instance, they measured for HCl , $\Delta H_{\text{sub}}(\text{HCl}) = 63.7 \text{ kJ mol}^{-1}$ (Thibert and Dominé, 1997) whereas $\Delta H_{\text{evap}}(\text{HCl})$ was about 74 kJ mol^{-1} (Fritz and Fuget, 1956). It is thus interesting that our value of ΔH_{sub} is fairly close to the partial molar enthalpy of evaporation of CH_3CHO : $\Delta H_{\text{evap}} = 52.2 \pm 0.2 \text{ kJ mol}^{-1}$ (Betterton and Hoffmann, 1988), suggesting that incorporation of CH_3CHO in a SSE is also a possibility. The winter values, that are lower than the spring fit, again suggest that either different incorporation mechanisms are involved in winter and spring or that there is an additional spring-time source of CH_3CHO in snow.

4.2.4. Solid solution ruled by condensation kinetics

We finally examined the hypothesis of the formation of a solid solution ruled by condensation kinetics (Eq. (3)). The mass accommodation coefficient of CH_3CHO on ice is unknown. To test the validity of Eq. (3), we calculated the ratio $\alpha_{\text{CH}_3\text{CHO}}/\alpha_{\text{H}_2\text{O}}$. If the hypothesis is correct, $\alpha_{\text{CH}_3\text{CHO}}/\alpha_{\text{H}_2\text{O}}$ should be the same for all snow layers, except for a possible temperature dependence. This ratio was calculated using $[\text{CH}_3\text{CHO}]_{\text{snow}}$ measured for two fresh snowfalls and one winter hoar frost samples. Assuming that, on 19 April, the very surface layer was mostly composed of

surface hoar, we also calculated the $\alpha_{\text{CH}_3\text{CHO}}/\alpha_{\text{H}_2\text{O}}$ ratio for that layer. Data for $P_{\text{H}_2\text{O}}$ were calculated at the elevation where the ice crystal formed, which was determined from temperature and relative humidity vertical profiles (Cabanes et al., 2002) and from ground values for surface hoar and hoar frost. The lack of CH_3CHO vertical profiles forced us to assume that $P_{\text{CH}_3\text{CHO}}$ at the height where the snow formed was similar to the ground value. Initial $[\text{CH}_3\text{CHO}]_{\text{snow}}$ for the 7 February (4W) snowfall was extrapolated to the date of the precipitation i.e. to ~ 4 ppbw on 7 February. Since the 13–14 April (7S) snowfall was first sampled a few hours after the snowfall the value determined on 14 April was used.

The calculated $\alpha_{\text{CH}_3\text{CHO}}/\alpha_{\text{H}_2\text{O}}$ ratios obtained for the 7 February and 13–14 April snowfalls were 0.0126 and 0.0339, respectively. Both these values are within a factor of 2.7 of each other which is reasonable considering the approximations made, especially on the vertical profile of CH_3CHO . The value obtained for the hoar frost of 16 February was 0.0023, while that for the surface hoar of 19 April was 0.0055. Both hoar values are within a factor of 2.3 of each other, which may also be considered reasonable, considering that $P_{\text{CH}_3\text{CHO}}$ right at the snow surface may have been different from the values measured 1 m (Guimbaud et al., 2002) or 2 m (Boudries et al., 2002) above the snow. However, hoar values and precipitating snow values differ by a factor of up to 15, implying that it is unlikely that $[\text{CH}_3\text{CHO}]_{\text{snow}}$ can be explained by condensation kinetics for both precipitating snow and surface hoar. This process may, however, apply to one of these snow types. According to Dominé and Thibert (1996), condensation kinetics is more likely to apply to fast growing ice. The growth rate of surface hoar is much slower than that of snow in the atmosphere. Several days were required to observe surface hoar crystals that reached the size of precipitating snow, that forms in a few hours, and we conclude that condensation kinetics may explain the composition of precipitating snow, but not that of surface hoar. This is consistent with the observation that on 19 April, the composition of the 7S layer was the same as that of both underlying 6S and 5S layers. On 19 April, this very surface layer was mostly composed of surface hoar (Cabanes et al., 2002) and its concentration is then close to the steady-state value of other layers, that may be the equilibrium value.

It is also noteworthy that $\alpha_{\text{CH}_3\text{CHO}}/\alpha_{\text{H}_2\text{O}}$ ratio for both fresh snow and surface hoar are higher in spring than in winter. Again, we come to the conclusion that either different processes are involved in winter and in spring, or that an additional process is involved in the spring.

4.2.5. Preliminary interpretations

In summary, the three incorporation mechanisms can each explain a fraction of the data. Surface incorpora-

tion is consistent with all the spring data. Equilibrium volume incorporation is consistent with steady-state concentrations of spring surface snow. Kinetic volume incorporation is consistent with fresh snow data. No single mechanism can explain all the data, indicating that a combination of these three mechanisms is involved or that processes not envisaged come into play. Given the lack of data on the physical parameters describing the interactions of CH_3CHO and ice, we cannot construct a valid incorporation model that would explain all the data. The presence of an extra source of CH_3CHO in the spring is suggested by most of our data (Figs. 4 and 5) and deserves further discussion.

Photolysis of an organic precursor is possible. From gas-phase measurements, Sumner and Shepson (1999) suggested that HCHO was photochemically produced in the snowpack and released to the atmosphere. One postulated mechanism was the oxidation of organics adsorbed on the surface or dissolved in the bulk of snow grains by radicals such as Cl or OH, that were photolytically produced in the snowpack. A similar photolytical source has been postulated for CH_3CHO or higher carbonyls, also based on gas-phase measurements (Guimbaud et al., 2002; Grannas et al., 2002; Boudries et al., 2002).

It is then strange that snow-phase measurements of HCHO do not indicate a photolytical source, while snow-phase measurements of CH_3CHO do. This could be due to the weak interaction of HCHO with the ice surface. HCHO produced on the surface would then be released to the gas phase, and will remain undetected in snow. This is consistent with the conclusion of Perrier et al. (2002) that HCHO is located in the ice volume, not on its surface. On the contrary, we suggest that CH_3CHO has a strong affinity for the ice surface, so that when CH_3CHO is photolytically produced on an ice surface, its residence time is sufficient to delay its release to the atmosphere. Since production is continuous in the spring, it leads to enhanced measured concentrations. One way to reconcile winter and spring data, as shown in Figs. 4 and 5, is to suggest that the correct value of $P_{\text{CH}_3\text{CHO}}$ in the spring would not be the atmospheric values, but the snowpack values. Guimbaud et al. (2002) show that snowpack values were up to 8 times higher than atmospheric ones in the spring. A factor of 5 would be sufficient to reconcile winter and spring data of Figs. 4 and 5. Because of the large uncertainties on $P_{\text{CH}_3\text{CHO}}$ in snow, caused by mixing with atmospheric air and other artefacts, this cannot be fully tested, but using the higher $P_{\text{CH}_3\text{CHO}}$ values in snow would include the photochemical production, and lead to the determination of equilibrium parameters valid for our whole data set.

It is even possible that CH_3CHO produced on the surface diffuses into the ice volume. Yet another possibility is that a precursor dissolved in the ice volume

yields CH_3CHO upon photolysis. Lastly, snow chemistry may be different in winter and spring, and melting spring snow for analysis could produce CH_3CHO by liquid-phase reaction of precursors that would be absent in the winter, due to the different atmospheric chemistry in the absence of sunlight. Although speculative, this may also explain why contamination problems were more severe in the spring.

4.3. Uptake mechanisms for acetone in snow

Our preliminary snow-phase acetone measurements are insufficient to discuss the incorporation mechanism of acetone in snow. Our data can be used to compare the affinities of CH_3CHO and $(\text{CH}_3)_2\text{CO}$ for ice. Mean spring $P_{(\text{CH}_3)_2\text{CO}}$ were ~ 700 pptv (12–24 April period), i.e. about 3–4 times the mean $P_{\text{CH}_3\text{CHO}}$. Values for $[(\text{CH}_3)_2\text{CO}]_{\text{snow}}$, however, were about half those of $[\text{CH}_3\text{CHO}]_{\text{snow}}$ for surface layers. So the apparent Henry's law coefficient of acetone in ice is a factor of 6–8 smaller than that of acetaldehyde. This may also indicate a smaller acetone photochemical production in ice. It is also noteworthy that crusted (6S) layer exhibited a 40% higher $[(\text{CH}_3)_2\text{CO}]_{\text{snow}}$ at midnight than at noon which is compatible with rapid exchanges with the atmosphere. This could be explained by temperature-sensitive processes such as adsorption/desorption but this is a preliminary conclusion.

5. Summary and conclusions

Acetaldehyde snow-phase concentrations were in the range 1–4 and 1–10 ppbw during the winter and spring campaigns, respectively. Snowpack acetaldehyde was shown to represent 67% and 94% of the (snow + ML) system in winter and spring, respectively. As also deduced for formaldehyde (Perrier et al., 2002), the snowpack then has the potential to impact CH_3CHO gas-phase concentrations. Acetone was measured for the first time in Arctic snow and concentrations of 1.5–3 ppbw were obtained in the spring.

The mechanism of incorporation of CH_3CHO in ice is probably the result of several processes. While CH_3CHO concentrations correlate well with snow SSA both in the winter and in the spring, incorporation of CH_3CHO on the ice surface only can be safely ruled out, as equilibration of the surface with the atmosphere is expected to be rapid, and the data of Figs. 4 and 5 show a difference between winter and spring that cannot be explained by adsorption only. The formation of a solid solution at equilibrium (SSE) cannot either explain all the data because spring-time concentrations are generally higher than winter time ones, which is contrary to thermodynamics. A spring-time photochemical source

of CH_3CHO in snow is a possible explanation of the spring/winter difference.

Many assumptions had to be made to reach these conclusions. Additional studies are required to reduce their impact. Vertical CH_3CHO profiles should be obtained. Analytical methods should also be improved. Contamination problems were encountered when measuring snow-phase acetaldehyde and its measurement in the atmosphere remains difficult. Acetone measurements in the snowpack must also be improved to allow an easier monitoring of its concentrations. Laboratory measurements of adsorption isotherms and mass accommodation coefficients of carbonyls on ice and their solubility and diffusion coefficients in the ice volume are necessary to interpret fully the present data, and to lead to a physical model of carbonyl/ice interactions that can describe air–snow exchange of carbonyls.

Acknowledgements

This work was supported by the French Polar Institute (IFRTP) and by CNRS through Programme National de Chimie Atmosphérique (PNCA).

References

- Bales, R.C., Choi, J., 1996. Conceptual framework for interpretation of exchange processes. In: Chemical Exchange Between the Atmosphere and Polar Snow Vol. 43, NATO ASI, Springer, Berlin, pp. 319–338.
- Barrie, L.A., Bottenheim, J.W., Schnell, R.C., Crutzen, P.J., Rasmussen, R.A., 1988. Ozone destruction and photochemical reactions at polar sunrise in the lower Arctic atmosphere. *Nature* 334, 138–141.
- Betterton, E.A., Hoffmann, M.R., 1988. Henry's law constants of some environmental important aldehydes. *Environmental Science and Technology* 22, 1415–1418.
- Bottenheim, J.W., Barrie, L.A., Heidt, L., Niki, H., Rasmussen, R.A., Shepson, P.B., 1990. Depletion of lower tropospheric ozone during Arctic spring: The Polar Sunrise Experiment 1988. *Journal of Geophysical Research* 95, 18555–18568.
- Bottenheim, J.W., Fuentes, J.D., Tarasick, D.W., Anlauf, K.G., 2002. Ozone in the Arctic lower troposphere during winter and spring 2000 (ALERT2000). *Atmospheric Environment* 36, 2535–2544.
- Boudries, H., Bottenheim, J.W., Guimbaud, C., Grannas, A.M., Shepson, P.B., Houdier, S., Perrier, S., Dominé, F., 2002. Distribution and trends of oxygenated hydrocarbons in the high Arctic derived from measurements in the atmospheric boundary layer and interstitial snow air during ALERT2000 field campaign. *Atmospheric Environment* 36, 2573–2583.
- Cabanes, A., Legagneux, L., Dominé, F., 2002. Evolution of the specific surface area and of crystal morphology of fresh snow near Alert during the ALERT2000 campaign. *Atmospheric Environment* 36, 2757–2777.

- Couch, T.L., Sumner, A.L., Dassau, T.M., Shepson, P.B., Honrath, R.E., 2000. An investigation of the interaction of carbonyl compounds with the snowpack. *Geophysical Research Letters* 27, 2241–2244.
- De Serves, C., 1994. Gas phase formaldehyde and peroxide measurements in the Arctic atmosphere. *Journal of Physical Research* 99, 25391–25398.
- Dominé, F., Thibert, E., 1996. Mechanism of incorporation of trace gases in ice grown from the gas phase. *Geophysical Research Letters* 23 (24), 3627–3630.
- Dominé, F., Thibert, E., Silvente, E., Legrand, M., Jaffrezo, J.-L., 1995. Determining past atmospheric HCl mixing ratios from ice core analyses. *Journal of Atmospheric Chemistry* 21, 165–186.
- Dominé, F., Cabanes, A., Taillandier, A.-S., Legagneux, L., 2001. Specific surface area of snow samples determined by CH₄ adsorption at 77 K, and estimated by optical microscopy and scanning electron microscopy. *Environmental Science and Technology* 35, 771–780.
- Dominé, F., Cabanes, A., Legagneux, L., 2002. Structure, microphysics, and surface area of the Arctic snowpack near alert during ALERT2000 field campaign. *Atmospheric Environment* 36, 2753–2765.
- Fritz, J.J., Fuget, C.R., 1956. Vapor pressure of aqueous hydrogen chloride solutions, 0° to 50°C. *Industrial English Chemistry, Chemical and Engineering Data Series* 1, 10–12.
- Grannas, A.M., Shepson, P.B., Guimbaud, C., Sumner, A.L., Albert, M., Simpson, W., Dominé, F., Boudries, H., Bottenheim, J.W., Beine, H., Honrath, R., Zhou, X., 2002. A study of photochemical and physical processes affecting carbonyl compounds in the Arctic atmospheric boundary layer. *Atmospheric Environment* 36, 2733–2742.
- Guimbaud, C., Grannas, A.M., Shepson, P.B., Boudries, H., Bottenheim, J.W., Fuentes, J.D., Dominé, F., Houdier, S., Perrier, S., Biesenthal, B., Splawn, B.G., 2002. Snowpack processing of acetaldehyde, acetone in the Arctic atmospheric boundary layer. *Atmospheric Environment* 36, 2473–2752.
- Hobbs, P.V., 1974. *Ice Physics*. Clarendon Press, Oxford.
- Honrath, R.E., Peterson, M.C., Guo, S., Dibb, J.E., Shepson, P.B., Campbell, B., 1999. Evidence of NO_x production within or upon ice particles in the Greenland snowpack. *Geophysical Research Letters* 26 (6), 695–698.
- Houdier, S., Perrier, S., Defrancq, E., Legrand, M., 2000. A new fluorescent probe for sensitive detection of carbonyl compounds: sensitivity improvement and application to environmental water samples. *Analytica Chimica Acta* 412, 221–233.
- Hutterli, M.A., Rothlisberger, R., Bales, R.C., 1999. Atmosphere-to-snow-to-firn transfer studies of HCHO at Summit, Greenland. *Geophysical Research Letters* 26, 1691–1694.
- Marbouty, D., 1980. An experimental study of temperature gradient metamorphism. *Journal of Glaciology* 26, 303–312.
- Perrier, S., Houdier, S., Dominé, F., Cabanes, A., Legagneux, L., Sumner, A.L., Shepson, P.B., 2002. Formaldehyde in arctic snow. Incorporation into ice particles and evolution in the snowpack. *Atmospheric Environment* 36, 2695–2705.
- Picaud, S., Toubin, C., Girardet, C., 2000. Monolayers of acetone and methanol on ice. *Surface Science* 454–456, 178–182.
- Schaff, J.E., Roberts, J.T., 1998. The adsorption of acetone on thin films of amorphous and crystalline ice. *Langmuir* 14, 1478–1486.
- Shepson, P.B., Sirju, A.-P., Hopper, J.F., Barrie, L.A., Young, V., Niki, H., Dryfhout, H., 1996. Sources and sinks of carbonyl compounds in the Arctic ocean boundary layer: Polar Ice Floe Experiment. *Journal of Geophysical Research* 101, 21081–21089.
- Sumner, A.L., Shepson, P.B., 1999. Snowpack production of formaldehyde and its effect on the Arctic troposphere. *Nature* 398, 230–233.
- Thibert, E., Dominé, F., 1997. Thermodynamics and kinetics of the solid solution of HCl in ice. *Journal of Physical Chemistry B* 101 (18), 3554–3565.
- Thibert, E., Dominé, F., 1998. Thermodynamics and kinetics of the solid state solution of HNO₃ in ice. *Journal of Physical Chemistry B* 102 (22), 4432–4439.
- Yokouchi, Y., Akimoto, H., Barrie, L.A., Bottenheim, J.W., Anlauf, K., Jobson, B.T., 1994. Serial gas chromatographic/mass spectrometric measurements of some volatile organic compounds in the Arctic atmosphere during the 1992 Polar Sunrise Experiment. *Journal of Geophysical Research* 99, 25379–25389.